IEEE Access
Multidisciplinary : Rapid Review : Open Access Journal

Received February 23, 2018, accepted March 22, 2018, date of publication March 26, 2018, date of current version April 23, 2018.

Digital Object Identifier 10.1109/ACCESS.2018.2819641

Design of Triplexer Using E-Stub-Loaded Composite Right-/Left-Handed Resonators and Quasi-Lumped Impedance Matching Network

KAI DA XU[1,2], (Member, IEEE), MENGZE LI[1,2], (Student Member, IEEE), YANHUI LIU[1,2], (Member, IEEE), YANG YANG[3], (Member, IEEE), AND QING HUO LIU[4], (Fellow, IEEE)

[1]Department of Electronic Science, Xiamen University, Xiamen 361005, China
[2]Shenzhen Research Institute, Xiamen University, Shenzhen 518057, China
[3]School of Electrical and Data Engineering, University of Technology Sydney, Ultimo, NSW 2007, Australia
[4]Department of Electrical and Computer Engineering, Duke University, Durham, NC 27708, USA

Corresponding author: Yanhui Liu (yanhuiliu@xmu.edu.cn)

This work was supported in part by the National Natural Science Foundation of China under Grant 61601390, in part by the Guangdong Natural Science Foundation under Grant 2016A030310375, and in part by the Shenzhen Science and Technology Innovation Project under Grant JCYJ20170306141249935.

ABSTRACT A compact triplexer based on E-stub-loaded composite right-/left-handed (ESL-CRLH) resonators with quasi-lumped impedance matching network is presented in this paper. The equivalent circuit model of the ESL-CRLH resonator is presented first and its left-/right-handed capacitance/inductance elements are fully derived. Then, a quasi-lumped impedance matching circuit is designed to connect the three ESL-CRLH resonator based filter channels for the triplexer construction. Finally, the designed triplexer obtains high isolations among the ports and low in-band insertion losses of the three filter channels centered at 1.86, 2.41, and 3.25 GHz, of which a miniaturized layout has been realized. Good agreement between the simulated and measured results can be observed to validate the design idea.

INDEX TERMS Bandpass filter, composite right-/left-handed transmission line (CRLH-TL), impedance matching circuit, stub loaded resonator, triplexer.

I. INTRODUCTION

Multiplexers play an important role for separating or combining different passband channels to accomplish the requirements of multi-band and multi-service communication systems. Many approaches have been investigated to achieve high performance of the multiplexers for practical applications, such as low passband loss in each channel, high isolation between channels and overall compact sizes [1]–[10]. One usual method is that adopting common-resonator configuration without use of input junction sections, which can miniaturize the circuit size [2], [3]. However, due to the modes limitation of the common resonator, it is hardly promoted to multiplexers with many channels, e.g., triplexers and quadruplexers. Another widely used method of the multiplexer design is employing distributed coupling technique to satisfy resonance conditions of all passband channels [4]–[9]. Therefore, matching conditions between common port and each in-band port need to be considered. To acquire more design freedom, constructing an impedance matching network to connect predesigned bandpass filters together [10]–[13] is a straightforward way to tune frequency responses of every passband, but at the expense of the overall size increase.

Composite right-/left-handed transmission line (CRLH-TL) [14], one of the most important realization methods of meta-materials, has been applied in many microwave components and circuits, such as filters [15], multiplexers [16], [17], and antennas [18] due to its inherent advantages in circuit miniaturizations. In [19], a planar diplexer based on CRLH-TL unit cells without lumped elements is presented, nevertheless, its size is still not compact enough and the calculated modeling details of the left-/right-handed capacitance/inductance elements are not available.

In this paper, a dual-mode E-stub-loaded composite right-/left-handed (ESL-CRLH) resonator and its equivalent circuit model are proposed and analyzed. Then, this resonator is employed for the design of three bandpass filters with different center frequencies. Finally, a quasi-lumped impedance matching network is designed to connect these three filter channels for the construction of a compact triplexer.

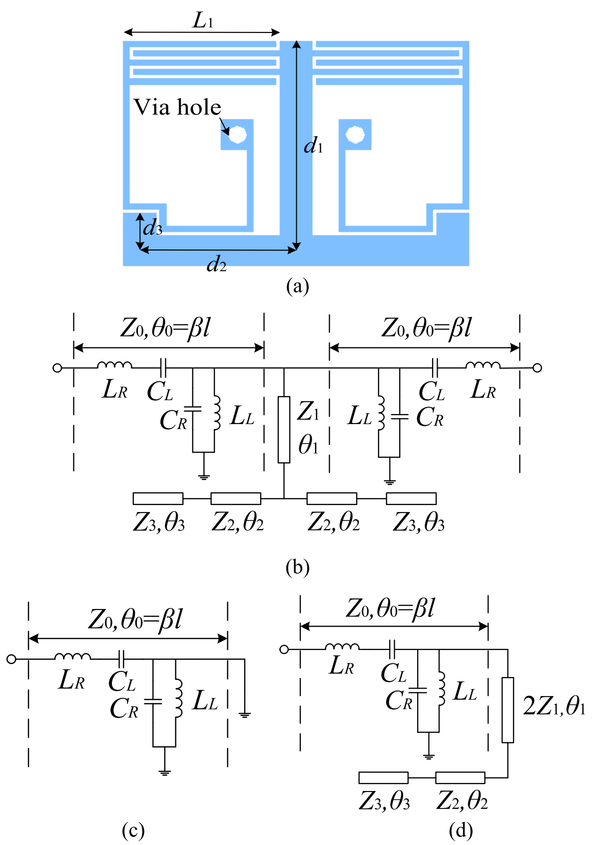

FIGURE 1. **(a) Layout and (b) equivalent circuit model of the ESL-CRLH resonator. (c) Odd-mode and (d) even-mode equivalent circuit model of the resonator.**

II. ESL-CRLH RESONATOR BASED FILTERS

As shown in Fig. 1(a), the proposed ESL-CRLH resonator consists of two symmetrically general CRLH-TL unit cells and a center loaded E-shaped stub. The compact construction makes a great contribution to layout miniaturization. Each CRLH-TL unit cell is composed of an interdigital capacitor and a shunt meandering short-circuited stub inductor, which can be equivalent to a left-handed (LH) capacitance (C_L) in series with a right-handed (RH) inductance (L_R) and a RH capacitance (C_R) in parallel with a LH inductance (L_L), respectively, as depicted in Fig. 1(b). Z_0 and θ_0 represent the equivalent characteristic impedance and electrical length of the CRLH-TL unit cell, respectively. Z_i, θ_i and d_i ($i = 1, 2, 3$) indicate their corresponding characteristic impedance, electrical length and physical length of E-shaped transmission-line stub, respectively.

The dispersion expression of phase shift over a CRLH-TL unit cell, i.e., θ_0, can be expressed by [20]

$$\theta_0 = \pm \arccos[1 - \frac{1}{2}(\omega^2 L_R C_R + 1/\omega^2 L_L C_L) + \frac{1}{2}(L_R/L_L + C_R/C_L)] \quad (1)$$

The sign "±" indicates negative when the CRLH-TL unit cell is in the LH band or positive in the RH band. If the length of CRLH-TL unit cell is smaller than quarter guided wavelength $l \leq \lambda_g/4$, i.e., $\theta_0 \leq \pi/2$, it can be seen as effectively homogeneous by electromagnetic waves [20].

Due to the symmetrical structure of the ESL-CRLH resonator, an odd- and even-mode method can be adopted to deduce its resonant properties. Fig. 1(c) shows the odd-mode equivalent circuit of the resonator and its odd-mode input impedance can be deduced as

$$Z_{in,odd} = jZ_0 \tan\theta_0 \quad (2)$$

Under the odd-mode excitation, the resonances will happen when $\theta_0 = (2n-1)\pi/2$ due to the resonance condition of $Z_{in,odd} = \infty$. The resonant angular frequency ω_{odd} can be deduced as

$$\omega_{odd} = 2\pi f_{odd} = \frac{(2n-1)\pi c}{2l\sqrt{\varepsilon_{eff}}} \quad (3)$$

where c denotes the velocity of light in free space, n is an integer, and ε_{eff} is the effective dielectric constant of the substrate. Taking the homogeneity condition into consideration, n should equal to 1, which means that the phase shift over the CRLH-TL unit cell is $\pi/2$ at ω_{odd}.

Similarly, the even-mode equivalent circuit of the ESL-CRLH resonator is exhibited in Fig. 1(d). To simplify the analysis, we assume $Z_0=2Z_1=Z_2=Z_3$. Thus, the input impedance of the even-mode equivalent circuit can be obtained as

$$Z_{in,even} = \frac{Z_0}{j\tan(\theta_0 + \theta_1 + \theta_2 + \theta_3)} \quad (4)$$

Due to the resonance condition of $Z_{in,even} = \infty$ under the even-mode excitation, the phase shift over the CRLH-TL unit cell and the loaded stub should be $n\pi$, i.e., $\theta_0 + \theta_1 + \theta_2 + \theta_3 = n\pi$. Therefore, the resonant angular frequency $\omega even$ can be obtained as:

$$\omega_{even} = 2\pi f_{even} = \frac{n\pi c}{(l + d_1 + d_2 + d_3)\sqrt{\varepsilon_{eff}}} \quad (5)$$

The LH/RH capacitances and inductances (i.e., C_L, C_R, L_L and L_R) can be calculated when the homogeneity condition is satisfied. Under the balanced frequency (ω_0), where θ_0 equals to zero, the four L and C elements have the following relationship

$$L_R C_L = L_L C_R = 1/\omega_0^2 \quad (6)$$

The characteristic impedance of the CRLH-TL unit cell at this balanced case is

$$Z_0 = \sqrt{L_L/C_L} = \sqrt{L_R/C_R} \quad (7)$$

Seen from the analysis above, for the odd-mode excitation, the phase shift over the CRLH-TL unit cell is $\pi/2$ at ω_{odd} and the dispersion relation is exhibited as follows

$$\frac{\pi}{2} = \pm \arccos[1 - \frac{1}{2}(\omega_{odd}^2 L_R C_R + 1/\omega_{odd}^2 L_L C_L) + \frac{1}{2}(L_R/L_L + C_R/C_L)] \quad (8)$$

For the even-mode excitation, the phase shift of the CRLH-TL unit cell and the loaded stub should be $n\pi$ at ω_{even}, i.e., $\theta_0+\theta_1+\theta_2+\theta_3 = n\pi$. Therefore, the dispersion relation of the unit cell can be expressed as

$$n\pi - \theta_1 - \theta_2 - \theta_3 = \pm \arccos[1 - \frac{1}{2}(\omega_{even}^2 L_R C_R + 1/\omega_{even}^2 L_L C_L) + \frac{1}{2}(L_R/L_L + C_R/C_L)] \quad (9)$$

Furthermore, θ_i ($i = 1, 2$ and 3) satisfies the following expression

$$\theta_1 + \theta_2 + \theta_3 = \beta(d_1 + d_2 + d_3) = \frac{\omega_{even}\sqrt{\varepsilon_{eff}}}{c}(d_1 + d_2 + d_3). \quad (10)$$

With the calculations of equations (6)-(10), the design formulas of C_L can be deduced by eliminating L_L, L_R and C_R at first (11a), as shown at the bottom of this page.

Then, the expressions of the other three L and C elements can be derived as(11b)–(11d), as shown at the bottom of this page.

Thus, the values of C_L, C_R, L_L and L_R can be calculated by using equation (11) for the solutions of the equivalent circuit model of the proposed ESL-CRLH resonator.

To validate the resonant frequencies can be tuned by the parameters of L_1, d_1, d_2 and d_3, two simulated frequency responses of the ESL-CRLH resonator based filter under weak coupling are illustrated in Fig. 2. When the length of L_1 increases from 3.3 to 3.9 mm, f_{odd} and f_{even} decline considerably as shown in Fig. 2(a), which means the center frequency of the filter $|f_{odd} + f_{even}|/2$ can be tuned flexibly by changing the length of the CRLH-TL unit cell. When d_3 increases from 1 to 2 mm, f_{odd} almost keeps unchanged, but f_{even} decreases as demonstrated in Fig. 2(b). Similarly, it will have the same result if the length of d_1 or d_2 varies. Consequently, these simulated results are in accordance with the above deduced equations (3) and (5). The electrical lengths of each CRLH-TL unit cell and center loaded E-stub can be regarded as a significant part initially for the filter design of a required passband using the proposed ESL-CRLH resonator.

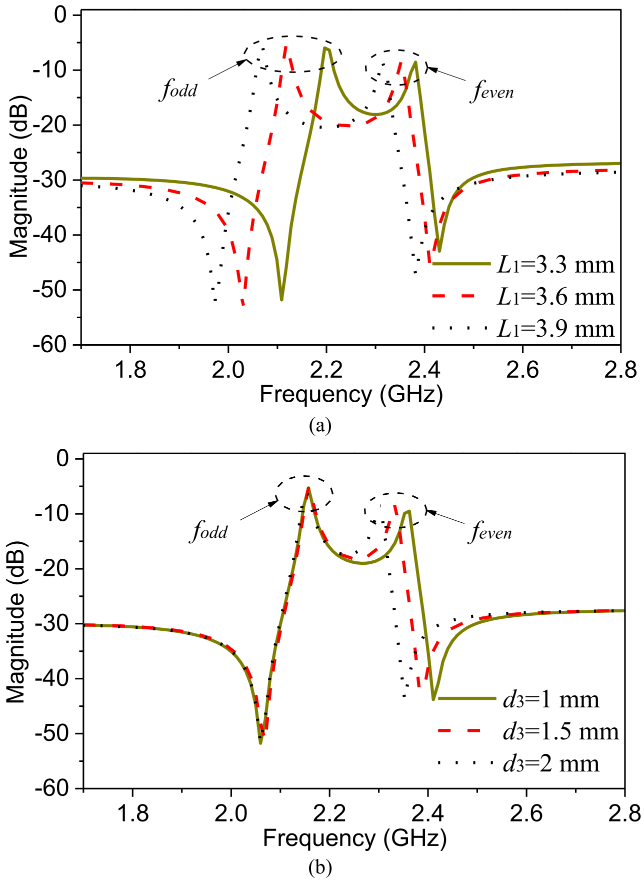

FIGURE 2. Simulated frequency responses of the proposed filter under weak coupling with varied (a) L_1 and (b) d_3.

Therefore, as illustrated in Fig. 3(a), the proposed ESL-CRLH resonator based filter is designed on a substrate with a relative dielectric constant of 3.48 and a thickness of 0.508 mm using full-wave electromagnetic simulator

$$C_L = \frac{\omega_{even}^2 - \omega_{odd}^2}{\omega_{odd}\omega_{even}Z_0[\sqrt{2}\omega_{even} - \omega_{odd}\sqrt{2+2\cos\frac{\omega_{even}\sqrt{\varepsilon_{eff}}}{c}(d_1+d_2+d_3)}]} \quad (11a)$$

$$L_L = \frac{Z_0(\omega_{even}^2 - \omega_{odd}^2)}{\omega_{odd}\omega_{even}(\sqrt{2}\omega_{even} - \omega_{odd}\sqrt{2+2\cos\frac{\omega_{even}\sqrt{\varepsilon_{eff}}}{c}(d_1+d_2+d_3)})]} \quad (11b)$$

$$C_R = \frac{\sqrt{2}\omega_{odd} - \omega_{even}\sqrt{2+2\cos\frac{\omega_{even}\sqrt{\varepsilon_{eff}}}{c}(d_1+d_2+d_3)}}{Z_0(\omega_{even}^2 - \omega_{odd}^2)} \quad (11c)$$

$$L_R = \frac{Z_0(\sqrt{2}\omega_{odd} - \omega_{even}\sqrt{2+2\cos\frac{\omega_{even}\sqrt{\varepsilon_{eff}}}{c}(d_1+d_2+d_3)}}{\omega_{even}^2 - \omega_{odd}^2} \quad (11d)$$

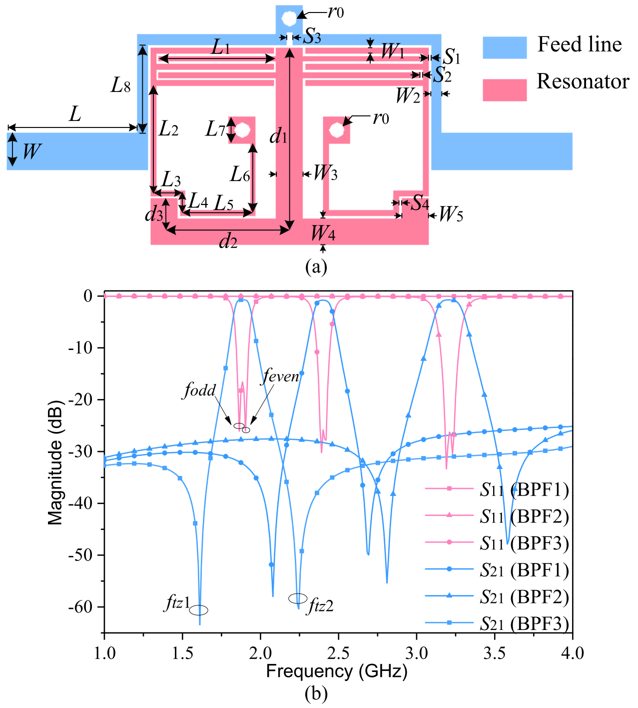

FIGURE 3. (a) Layout of the proposed ESL-CRLH resonator based filter. (b) Simulated frequency responses of three BPFs with center frequencies at 1.8, 2.4, and 3.2 GHz, respectively.

HFSS [21]. Magnetic source-load cross coupling is employed to achieve high frequency selectivity of the filter. Three BPFs with different center frequencies are designed in order to construct a required triplexer which is presented in Section III. Fig. 3(b) shows the simulated frequency responses of these three BPFs (i.e., BPF1, BPF2 and BPF3) with center frequencies at 1.8, 2.4, and 3.2 GHz, respectively, each of which has two transmission poles and two transmission zeros. Taking BPF1 with center frequency at 1.8 GHz for instance, it possesses two resonant frequencies (i.e., f_{odd} and f_{even}) and two transmission zeros (i.e., f_{tz1} and f_{tz2}). These two transmission zeros are introduced at either side of the passband with more than 60 dB attenuations. The passbands of BPF1, BPF2 and BPF3 have the 3-dB fractional bandwidths of 6.5%, 5.7% and 5.8%, respectively. All insertion losses of these three BPFs are less than 0.8 dB and all stopbands obtain the rejection levels of better than 25 dB. Table 1 tabulates physical dimensions of these three BPFs and their corresponding characteristics.

Once the parameters of the ESL-CRLH resonator are fixed, i.e., two resonances f_{odd} and f_{even} remain unchanged, the bandwidth of the filter is mainly determined by the external quality factor Q_e. Fig. 4 shows the variation of Q_e against different values of L_8. As the length of feed line L_8 increases from 1.5 to 4.5 mm, the Q_e decreases significantly. Therefore, the required passband bandwidth of the filter can be tuned by the parameter L_8.

Compare with the single-mode CRLH-TL resonator in [16], the proposed ESL-CRLH resonator consisting of

TABLE 1. Physical dimensions and performance of BPF1, BPF2 and BPF3.

	CF (GHz)	IL (dB)	RL (dB)	FBW (%)	Number of TZs	Circuit size $\lambda_g \times \lambda_g$
BPF1	1.8	0.74	16.5	6.5	2	0.12×0.08
	Dimensions (Unit: mm): W=1.1, W_1=0.15, W_2=0.3, L=4, L_1=5, L_2=2.4, L_3=0.9, L_4=1.8, L_5=3, L_6=2.65, L_8=3.9, S_1=S_2=S_4=0.1, S_3=0.2, d_1=5.6, d_2=5.65, d_3=2.2, r_0=0.25, W_3=W_4=W_5=L_7=0.8. LH/RH C/L elements: C_L=1 pF, L_L=2.5 nH, C_R=0.3 pF, L_R=0.8 nH.					
BPF2	2.4	0.8	25.7	5.7	2	0.12×0.09
	Dimensions (Unit: mm): W=1.1, W_1=0.15, W_2=0.3, L=4, L_1=3.6, L_2=3.2, L_3=0.9, L_4=0.6, L_5=2, L_6=2.05, L_8=2.7, S_1=S_2=S_4=0.1, S_3=0.2, d_1=5.2, d_2=4.25, d_3=1, r_0=0.25, W_3=W_4=W_5=L_7=0.8. LH/RH C/L elements: C_L=0.6 pF, L_L=1.5 nH, C_R=1 pF, L_R=2.5 nH.					
BPF3	3.2	0.75	26.9	5.8	2	0.13×0.11
	Dimensions (Unit: mm): W=1.1, W_1=0.15, W_2=0.3, L=4, L_1=2.7, L_2=2.4, L_3=0.9, L_4=0.4, L_5=1, L_6=1.65, L_8=2.1, S_1=S_2=S_4=0.1, S_3=0.2, d_1=4.2, d_2=3.35, d_3=0.8, r_0=0.25, W_3=W_4=W_5=L_7=0.8. LH/RH C/L elements: C_L=0.5 pF, L_L=1.3 nH, C_R=0.7 pF, L_R=1.8 nH.					

CF, IL, RL, TZ and FBW denote center frequency, insertion loss, return loss, transmission zero and fractional bandwidth, respectively.

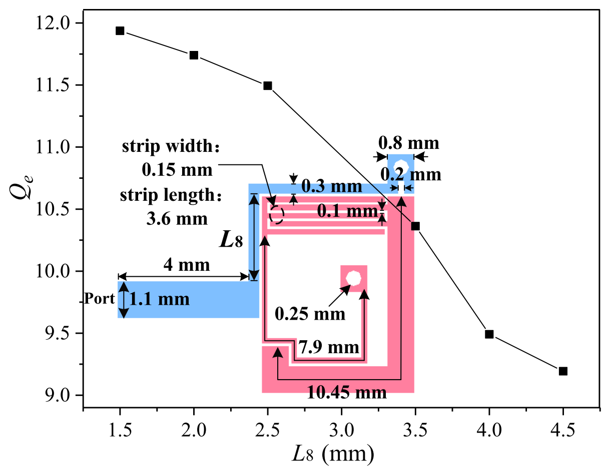

FIGURE 4. Extracted external quality factor Q_e against varied L_8.

two symmetrically general CRLH-TL unit cells and a center loaded E-shaped stub has two resonant modes, which can be analyzed by the odd- and even-mode method. Although two CRLH-TL unit cells need to be employed in the resonator, the even-mode resonant frequency can be adjusted by the length of the E-shaped stub. Thus, the bandwidth of the BPF can be further tuned even if the feedline coupling type and external quality factor are fixed. In contrast, the resonant modes in the traditional CRLH-TL resonator (e.g. resonator in [16]) can be hardly tuned unless the LC values of C_L, C_R, L_L and L_R are changed. Therefore, the bandwidths of the proposed resonator-based filter with two resonant modes (6.5% of BPF1, 5.7% of BPF2, and 5.8% of BPF3) are even wider than that of the fourth-order filter using four resonators with four resonant modes (only 5%) in [16].

III. TRIPLEXER DESIGN

Fig. 5 shows the schematic of the proposed triplexer and its physical realization on the printed circuit board. After the design of three BPFs as seen in Fig. 3, the corresponding s2p files are extracted from their electromagnetic simulated results. There are three passband channels,

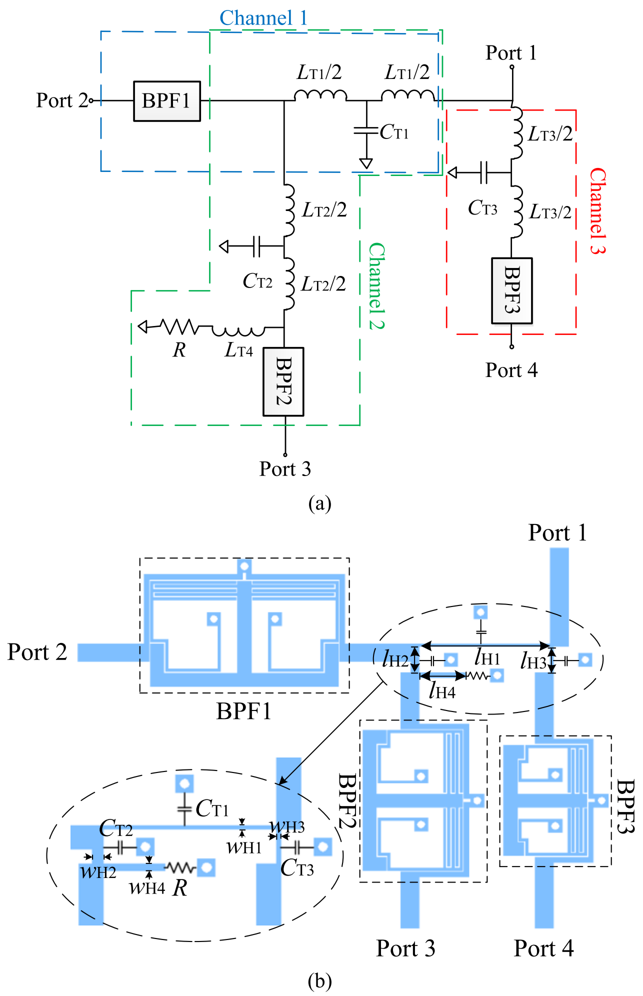

FIGURE 5. **(a) Schematic and (b) physical layout of the proposed triplexer.**

i.e., Channels 1, 2 and 3, as illustrated in Fig. 5(a), and an impedance matching circuit consisting of three T-shaped LC-networks is constructed to achieve the desired impedance matching condition. A series L_{T4}-R tank to the ground is shunted to the Channel 2 after the T-shaped LC-network, which is in order to absorb the harmonic frequency responses [22], [23].

The capacitances C_{Ti} can be realized by using lumped capacitors, while the inductances L_{Ti} can be achieved by using high-impedance microstrip lines with lengths of l_{Hi} and widths of w_{Hi} (i = 1, 2, 3, and 4) as seen in Fig. 5(b), which can be calculated by the following empirical formulas [24]

$$L_{Ti}(\text{nH}) = 2 \times 10^{-7} k l_{Hi} \times \ln\left(\frac{l_{Hi}}{w_{Hi}+t} + 1.193 + \frac{w_{Hi}+t}{3l_{Hi}}\right) \tag{12a}$$

$$k = 0.57 - 0.145 \ln(w_{Hi}/h), \quad w_{Hi}/h > 0.05 \tag{12b}$$

where t and h are the metal thickness of microstrip line and the substrate thickness, respectively.

The overall circuit of the triplexer is optimized using ADS software [25] through importing the extracted BPF

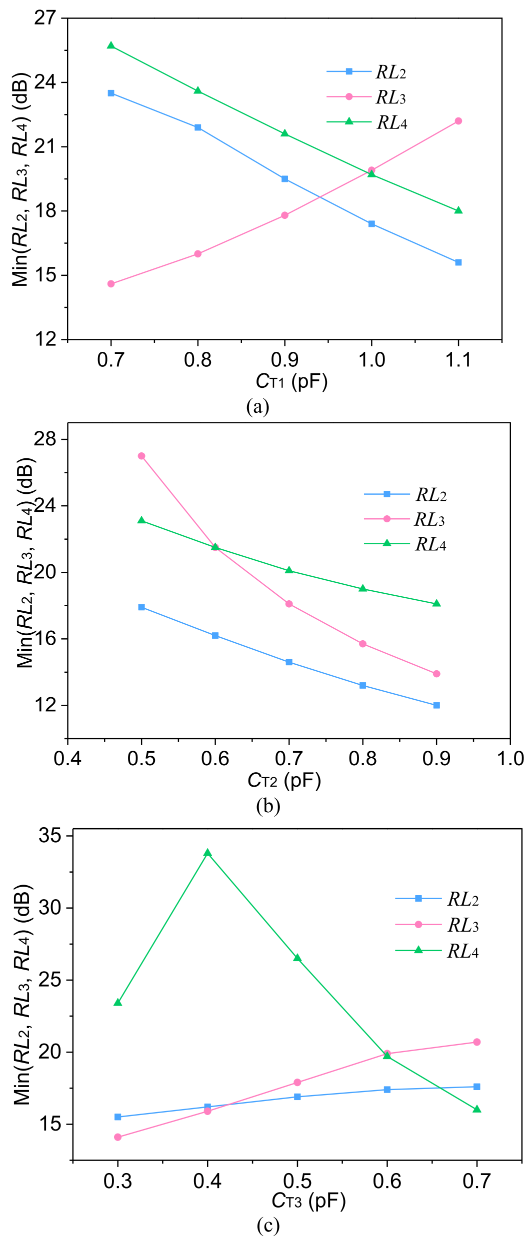

FIGURE 6. **Variation of Min(RL_2, RL_3, RL_4) against (a) C_{T1}, (b) C_{T2} and (c) C_{T3}.**

s2p files from HFSS simulator. The final optimized parameters in Fig. 5(a) are chosen as follows: $C_{T1} = 1$ pF, $C_{T2} = C_{T3} = 0.6$ pF, $L_{T1} = 4.5$ nH, $L_{T2} = 0.27$ nH, $L_{T3} = 0.48$ nH, $L_{T4} = 0.82$ nH, and $R = 5.1$ kΩ. Therefore, according to (12), the lengths and widths of the four high-impedance microstrip lines can be taken as: $w_{H1} = 0.18$ mm and $l_{H1} = 8.4$ mm, $w_{H2} = 0.5$ mm and $l_{H2} = 1.6$ mm, $w_{H3} = 0.2$ mm and $l_{H3} = 1.6$ mm, $w_{H4} = 0.3$ mm and $l_{H4} = 2.8$ mm, respectively. Fig. 6 illustrates the variation of Min(RL_2, RL_3, RL_4) against C_{T1}, C_{T2}, and C_{T3}, where RL_2, RL_3, and RL_4 represent the return losses of output ports 2, 3, and 4, respectively, and Min(RL_2, RL_3, RL_4) denotes the minimum values of RL_2, RL_3, and RL_4. From Fig. 6(a), it can be observed that RL_3 becomes better but RL_2

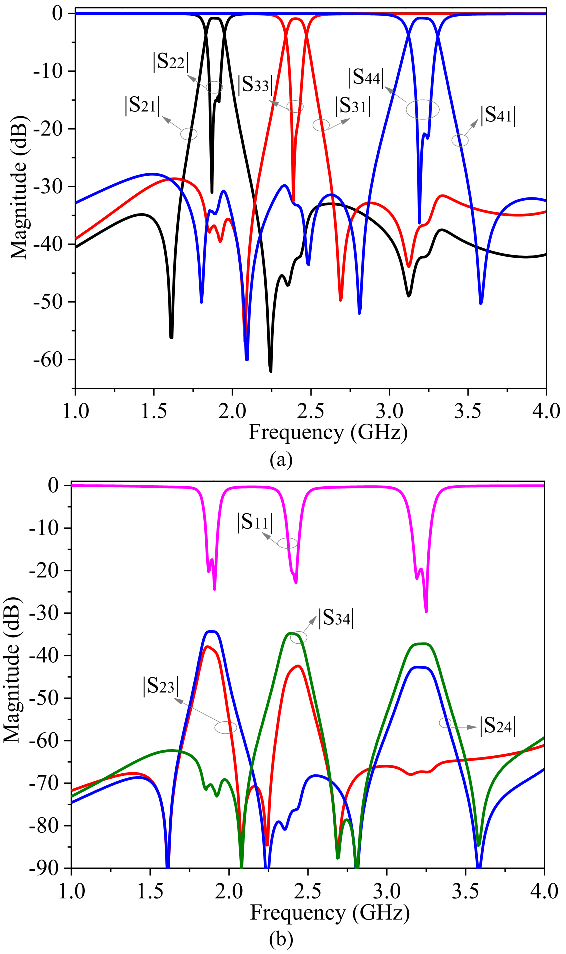

FIGURE 7. ADS Simulated results of the triplexer. (a) $|S_{21}|$, $|S_{22}|$, $|S_{31}|$, $|S_{33}|$, $|S_{41}|$, and $|S_{44}|$. (b) $|S_{11}|$, $|S_{23}|$, $|S_{34}|$, and $|S_{24}|$.

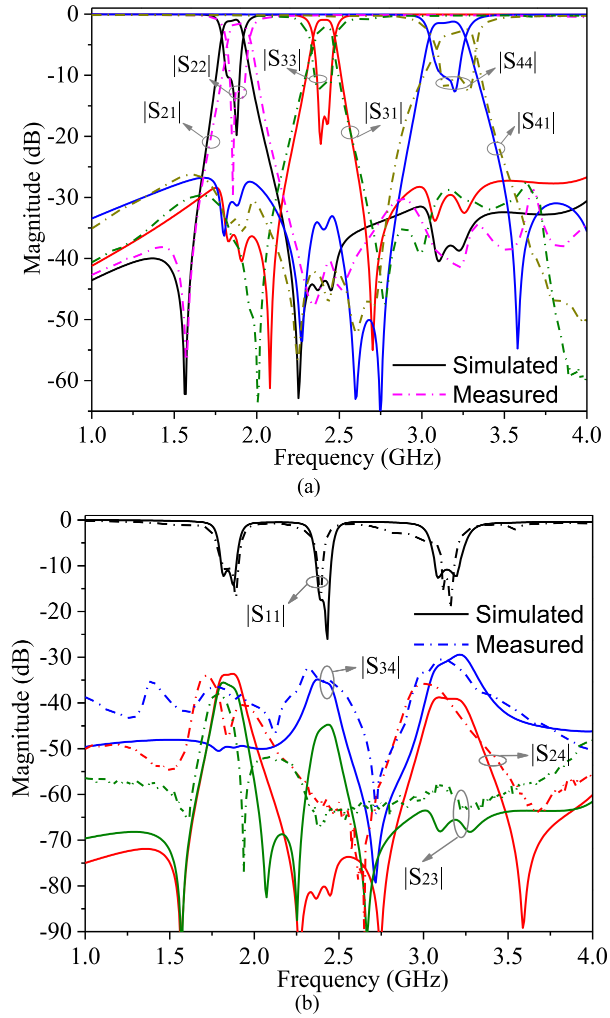

FIGURE 8. HFSS simulations and measurements of the triplexer. (a) $|S_{21}|$, $|S_{22}|$, $|S_{31}|$, $|S_{33}|$, $|S_{41}|$, and $|S_{44}|$. (b) $|S_{11}|$, $|S_{23}|$, $|S_{34}|$, and $|S_{24}|$.

and RL_4 will be worse when the value of C_{T1} increases from 0.7 to 1.1 pF. Fig. 6(b) illustrates that all of the RL_2, RL_3 and RL_4 will decrease as C_{T2} rises from 0.5 to 0.9 pF. For the C_{T3} as shown in Fig. 6(a), the RL_2 and RL_3 will change slightly, but RL_4 will first rise up and then fall down when C_{T3} increases. To make a trade-off among these return losses of three output ports, the three lumped capacitors are finally chosen as $C_{T1} = 1$ pF and $C_{T2} = C_{T3} = 0.6$ pF, respectively.

Fig. 7 illustrates the simulated results carried by ADS software, and Fig. 8 shows the measured S-parameters of the triplexer as well as the simulated ones using HFSS simulator, which are basically in agreement. The differences between simulated and measured results may be attributed to the fabrication error and soldering of the SMA connectors. Additionally, due to the fact that the SMT capacitors have intrinsic disadvantage of higher losses working at higher frequencies, the capacitors C_{T2} and C_{T3} used in the Channels 2 and 3 may cause relatively large insertion losses within the passbands.

It is observed that the measured center frequencies of the three channels are at 1.86, 2.41 and 3.25 GHz, and their fractional bandwidths are of 7.5%, 5.3% and 6.8%, respectively. Fig. 9 shows the photograph of the fabricated triplexer. The overall circuit size is of 19.3 mm × 28 mm excluding the input/output ports, i.e., $0.19\lambda_g \times 0.28\lambda_g$, where λ_g is the guided wavelength of the 50 Ω microstrip line at the first center frequency. Table 2 summarizes the comparisons with other reported multiplexers, which shows the proposed triplexer has low in-band insertion losses, high isolations and very compact size.

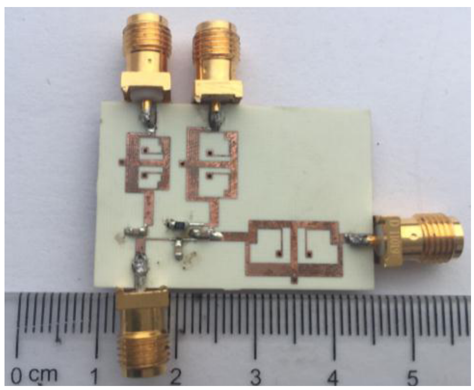

FIGURE 9. Photograph of the fabricated triplexer.

TABLE 2. Comparisons with some previous multiplexers

	CF (GHz)	Minimum IL (dB)	FBW (%)	Isolation (dB)	Size (λ_g^2)
[2]	1.1, 1.3	1.83, 1.52	8.0, 9.2	>26	0.82×0.86
[1]	3.38, 3.89, 4.56	2.2, 2.3, 2.3	16.2, 13, 16	>15	0.52×0.52
[3]	3.2, 3.7, 4.4	2.7, 2.5, 1.8	6.6, 7.3, 8.2	>35	0.20×0.67
[10]	1.5, 1.7, 1.9	4.94, 5.82, 5.95	3.33, 2.94, 2.63	>50	0.65×0.57
[17]-II	1.8, 2.38, 3.73	1.3, 1.4, 1.7	Not Given	>25	0.15×0.22
This work	**1.86, 2.41, 3.25**	**1.5, 2.1, 2.45**	**7.5, 5.3, 6.8**	**>30**	**0.19×0.28**

IV. CONCLUSION

In this paper, the resonant performance and LH/RH capacitance/inductance element deductions of the ESL-CRLH resonator are analyzed. Then three size-different BPFs using ESL-CRLH resonators and a quasi-lumped impedance matching network are designed to construct a miniaturized triplexer. Low in-band insertion losses and high isolations among the three filter channels are obtained for the triplexer, which can be a promising candidate for modern multi-standard communication systems.

REFERENCES

[1] C. W. Tang and M. G. Chen, "Packaged microstrip triplexer with star-junction topology," *Electron. Lett.*, vol. 48, no. 12, pp. 699–700, Jun. 2012.

[2] D. Chen, L. Zhu, H. Bu, and C. Cheng, "A novel planar diplexer using slotline-loaded microstrip ring resonator," *IEEE Microw. Wireless Compon. Lett.*, vol. 25, no. 11, pp. 706–708, Nov. 2015.

[3] J.-Y. Wu, K.-W. Hsu, Y.-H. Tseng, and W.-H. Tu, "High-isolation microstrip triplexer using multiple-mode resonators," *IEEE Microw. Wireless Compon. Lett.*, vol. 22, no. 4, pp. 173–175, Apr. 2012.

[4] J.-Y. Wu, Y.-H. Tseng, and W.-H. Tu, "Packaged triplexer based on distributed coupling technique," *IEEE Microw. Mag.*, vol. 13, no. 1, pp. 139–145, Jan./Feb. 2012.

[5] W. Feng, Y. Zhang, and W. Che, "Tunable dual-band filter and diplexer based on folded open loop ring resonators," *IEEE Trans. Circuits Syst. II, Exp. Briefs*, vol. 64, no. 9, pp. 1047–1051, Sep. 2017.

[6] F.-C. Chen, J.-M. Qiu, H.-T. Hu, Q.-X. Chu, and M. J. Lancaster, "Design of microstrip lowpass-bandpass triplexer with high isolation," *IEEE Microw. Wireless Compon. Lett.*, vol. 25, no. 12, pp. 805–807, Dec. 2015.

[7] W. Feng, X. Gao, and W. Che, "Microstrip diplexer for GSM and WLAN bands using common shorted stubs," *Electron. Lett.*, vol. 50, no. 20, pp. 1486–1488, Sep. 2014.

[8] W.-H. Tu and C.-L. Wu, "Design of microstrip low-pass-bandpass multiplexers using distributed coupling technique," *IEEE Trans. Compon., Packag., Manuf. Technol.*, vol. 6, no. 11, pp. 1648–1655, Nov. 2016.

[9] H.-W. Hsu and W.-H. Tu, "Microwave microstrip six-channel triplexer and eight-channel quadruplexer," *IEEE Trans. Compon., Packag., Manuf. Technol.*, vol. 7, no. 7, pp. 1136–1143, Jul. 2017.

[10] S.-C. Lin and C.-Y. Yeh, "Design of microstrip triplexer with high isolation based on parallel coupled-line filters using T-shaped short-circuited resonators," *IEEE Microw. Wireless Compon. Lett.*, vol. 25, no. 10, pp. 648–650, Oct. 2015.

[11] J. Xu and Y. Zhu, "Microstrip triplexer and switchable triplexer using new impedance matching circuits," *Int. J. RF Microw. Comput. Aided Eng.*, vol. 27, p. e21057, Oct. 2017.

[12] S. Taravati and M. Khalaj-Amirhosseini, "Design method for matching circuits of general multiplexers," *IET Microw., Antennas Propag.*, vol. 7, no. 4, pp. 237–244, Mar. 2013.

[13] P.-H. Deng, B.-L. Huang, and B.-L. Chen, "Designs of microstrip four- and five-channel multiplexers using branch-line-shaped matching circuits," *IEEE Trans. Compon., Packag., Manuf. Technol.*, vol. 5, no. 9, pp. 1331–1338, Sep. 2015.

[14] A. Lai, T. Itoh, and C. Caloz, "Composite right/left handed transmission line metamaterials," *IEEE Microw. Mag.*, vol. 5, no. 3, pp. 34–50, Mar. 2004.

[15] G. Shen, W. Che, W. Feng, and Q. Xue, "Analytical design of compact dual-band filters using dual composite right-/left-handed resonators," *IEEE Trans. Microw. Theory Techn.*, vol. 65, no. 3, pp. 804–814, Mar. 2017.

[16] T. Yang, P.-L. Chi, and T. Itoh, "High isolation and compact diplexer using the hybrid resonators," *IEEE Microw. Wireless Compon. Lett.*, vol. 20, no. 10, pp. 551–553, Oct. 2010.

[17] T. Yang, P.-L. Chi, and T. Itoh, "Compact quarter-wave resonator and its applications to miniaturized diplexer and triplexer," *IEEE Trans. Microw. Theory Techn.*, vol. 59, no. 2, pp. 260–269, Feb. 2011.

[18] B. F. Zong, G. M. Wang, Y. W. Wang, and L. Geng, "Compact antenna using finger-connected interdigital capacitor-based composite right/left-handed transmission-line unit cell," *IEEE Trans. Antennas Propag.*, vol. 64, no. 5, pp. 1994–1999, 2016.

[19] H. Y. Zeng, G. M. Wang, D. Z. Wei, and Y. W. Wang, "Planar diplexer using composite right-/left-handed transmission line under balanced condition," *Electron. Lett.*, vol. 48, no. 2, pp. 104–105, 2012.

[20] C. Caloz and T. Itoh, *Electromagnetic Metamaterials: Transmission Line Theory and Microwave Applications*. New York, NY, USA: Wiley, 2004.

[21] ANSYS Corp. (2012). *ANSYS High Frequency Structure Simulator (HFSS), Ver. 13.0*. [Online]. Available: www.ansoft.com

[22] C. J. Galbraith, R. D. White, L. Cheng, K. Grosh, and G. M. Rebeiz, "Cochlea-based RF channelizing filters," *IEEE Trans. Circuits Syst. I, Reg. Papers*, vol. 55, no. 4, pp. 969–979, Apr. 2008.

[23] C. J. Galbraith and G. M. Rebeiz, "Higher order cochlea-like channelizing filters," *IEEE Trans. Microw. Theory Techn.*, vol. 56, no. 7, pp. 1675–1683, Jul. 2008.

[24] I. Bahl, *Lumped Elements for RF and Microwave Circuits*. Boston, MA, USA: Artech House, 2003.

[25] *Advanced Design System (ADS) Student*, Agilent Tech, Inc., Santa Clara, CA, USA, 2013.

KAI DA XU (S'13–M'15) received the B.S. and Ph.D. degrees in electromagnetic field and microwave technology from the University of Electronic Science and Technology of China (UESTC), Chengdu, China, in 2009 and 2015, respectively.

From 2012 to 2014, he was a Visiting Researcher with the Department of Electrical and Computer Engineering, Duke University, Durham, NC, USA, under the financial support from the China Scholarship Council. From 2016 to 2017, he was a Post-Doctoral Fellow with the State Key Laboratory of Millimeter Waves, City University of Hong Kong, Hong Kong. He is currently an Assistant Professor with the Institute of Electromagnetics and Acoustics and the Department of Electronic Science, Xiamen University, Xiamen, China. He has authored and co-authored over 80 papers in peer-reviewed journals and conference proceedings. His current research interests include RF/microwave and mm-wave circuits, antenna arrays, and nanoscale memristors.

Dr. Xu received the UESTC Outstanding Graduate Awards in 2009 and 2015. He was a recipient of the National Graduate Student Scholarship from the Ministry of Education, China, in 2012, 2013, and 2014. He is serving as a Reviewer for several IEEE and IET journals, including the IEEE TRANSACTIONS ON MICROWAVE THEORY AND TECHNIQUES, the IEEE TRANSACTIONS ON ELECTRON DEVICES, the IEEE TRANSACTIONS ON COMPUTER-AGIDED DESIGN OF INTEGRATED CIRCUITS AND SYSTEMS, the *IEEE Microwave Magazine*, the IEEE ANTENNAS AND WIRELESS PROPAGATION LETTERS, the IEEE MICROWAVE AND WIRELESS COMPONENTS LETTERS, the IEEE ACCESS, *IET Microwaves Antennas and Propagation*, and *Electronics Letters*. Since 2017, he has served as an Associate Editor for the IEEE ACCESS and *Electronics Letters*. He is also an Editorial Board Member of the *AEÜ-International Journal of Electronics and Communications*.

MENGZE LI was born in Hunan, China, in 1994. She received the B.Eng. degree in electrical engineering and automation from Hunan University, Hunan, China, in 2015.

She is currently pursuing the M.Eng. degree with Xiamen University, Xiamen, China. Since 2017, she has been a Visiting Student with the University of Technology Sydney, under the financial support from the China Scholarship Council. Her current research interests include microstrip filters, multiplexers, and RFIC.

YANHUI LIU (M'15) received the B.S. and Ph.D. degrees in electrical engineering from the University of Electronic Science and Technology of China (UESTC), Sichuan, China, in 2004 and 2009, respectively.

From 2007 to 2009, he was a Visiting Scholar with the Department of Electrical Engineering, Duke University, Durham, NC, USA. Since 2011, he has been with Xiamen University, China, where he is currently a Full Professor with the Department of Electronic Science. In 2017, he was a Visiting Professor with the State Key Laboratory of Millimeter Waves, City University of Hong Kong. He has authored and co-authored over 110 peer-reviewed journal and conference papers. He holds several granted Chinese patents. His research interests include antenna array design, array signal processing, and microwave imaging methods. He received the UESTC Outstanding Graduate Award in 2004 and the Excellent Doctoral Dissertation Award of Sichuan Province of China in 2012. He is serving as a Reviewer for several international journals including the IEEE Transactions on Antennas and Propagation, the IEEE Transactions on Geosciences and Remote Sensing, the IEEE Antennas and Wireless Propagation Letters, the IEEE Microwave and Wireless Components Letters, the *IET Microwave, Antennas and Propagation*, and *Digital Signal Processing*. Since 2018, he has served as an Associate Editor for the IEEE Access.

YANG YANG (S'11–M'14) was born in Inner Mongolia, China. He received the Ph.D. degree from Monash University, Clayton, VIC, Australia, in 2013. From 2012 to 2015, he was an Asia Pacific GSP Engineer at Rain Bird and the Global GSP Success Award holder of the year 2014. From 2015 to 2016, he served as a Senior Research Associate with the Department of Engineering, Macquarie University, Sydney, NSW, Australia.

From 2016 to 2016, he was a Research Fellow with the State Key Laboratory of Millimeter-Waves, City University of Hong Kong. In 2016, he was involved in the National Basic Research Program of China (973 Program) and appointed as an Honorary Research Fellow with the Shenzhen Institute, City University of Hong Kong. In 2016, he joined the University of Technology Sydney, Ultimo, NSW, Australia, as a Lecturer. His research interests include RFIC, microwave and millimeter-wave circuits and systems, reconfigurable antennas, wearable antennas, and wearable medical sensing devices and systems.

QING HUO LIU (S'88–M'89–SM'94–F'05) received the B.S. and M.S. degrees in physics from Xiamen University, China, and the Ph.D. degree in electrical engineering from the University of Illinois at Urbana-Champaign.

He has published over 400 papers in refereed journals and 500 papers in conference proceedings. His research interests include computational electromagnetics and acoustics, inverse problems, and their application in nanophotonics, geophysics, biomedical imaging, and electronic packaging. He was with the Electromagnetics Laboratory, University of Illinois at Urbana-Champaign, as a Research Assistant from 1986 to 1988, and as a Post-Doctoral Research Associate from 1989 to 1990. He was a Research Scientist and the Program Leader with Schlumberger-Doll Research, Ridgefield, CT, USA, from 1990 to 1995. From 1996 to 1999, he was an Associate Professor with New Mexico State University. Since 1999, he has been with Duke University, where he is currently a Professor of electrical and computer engineering.

Dr. Liu is a fellow of the Acoustical Society of America, the Electromagnetics Academy, and the Optical Society of America. He received the 1996 Presidential Early Career Award for Scientists and Engineers from the White House, the 1996 Early Career Research Award from the Environmental Protection Agency, and the 1997 CAREER Award from the National Science Foundation. He received the ACES Technical Achievement Award in 2017. He serves as an IEEE Antennas and Propagation Society Distinguished Lecturer from 2014 to 2016. He currently serves as the founding Editor-in-Chief of the new IEEE Journal on Multiscale and Multiphysics Computational Techniques, the Deputy Editor-in-Chief of the *Progress in Electromagnetics Research*, and an Editor of the *Journal of Computational Acoustics*.